Int. J. Heat Mass Transfer. Vol. 11, pp. 1013–1026. Pergamon Press 1968. Printed in Great Britain

TRANSPORT PROCESSES IN FLOW AROUND A SPHERE WITH PARTICULAR REFERENCE TO THE TRANSFER OF MASS

K. LEE† and H. BARROW‡

(*Received* 9 *June* 1967 *and in revised form* 8 *December* 1967)

Abstract—In the present study, the integrated boundary-layer equations are solved to calculate the development of the diffusion (or thermal) boundary layer from the forward stagnation point of a sphere up to the point of separation, for various values of the Schmidt (or Prandtl) number. The Pohlhausen polynomial profiles are used to describe the shapes of the transfer layers in the laminar region.

A method of "dry spraying" of napthalene was used to determine the local Sherwood number experimentally for Reynolds numbers between 3199 and 25350.

The experimental results for the laminar region are compared with those according to the theory. For the wake, a study of the experimental data shows that it is possible to specify three separate regimes corresponding to different Reynolds number ranges.

The present results are combined with those of other experimenters in heat and mass transfer to obtain an overall transfer coefficient from a sphere for a Reynolds number range of 200–200000.

NOMENCLATURE

b, concentration difference of species 1 $(= w_1 - w_{1w})$;
c, specific heat at constant pressure;
D, diffusion coefficient;
d, diameter;
$f, f_1, f_2 \ldots f^*, g^*$, functions as defined in text;
h, heat-transfer coefficient;
h_D, mass-transfer coefficient;
k, thermal conductivity;
R, radius;
r, radius of transverse cross section of body of revolution;
t, temperature;
U, velocity at edge of boundary layer;
u, velocity in x direction;
w, mass fraction;
$x, (y)$, distance along (and normal to) surface;
y', dimensionless distance $(= y/d)$;
Z, dimensionless parameter $(= U_\infty \delta^2/Rv)$;
Nu, Nusselt number $(= hd/k)$;
Pr, Prandtl number $(= c\mu/k)$;
Re, Reynolds number $(= U_\infty d/v)$;
Sh, Sherwood number $(= h_D d/D)$;
Sc, Schmidt number $(= v/D)$;

Greek symbols

α, thermal diffusivity $(= k/c\rho)$;
β, dimensionless concentration difference parameter $(= b/b_s)$;
δ, thickness of velocity boundary layer;
Δ, thickness of diffusion or thermal boundary layer;
λ, form parameter of velocity profile $[= \delta^2(\mathrm{d}U/\mathrm{d}x)/v]$;
θ, temperature difference $(= t - t_w)$;
θ', dimensional temperature difference parameter $(= \theta/\theta_s)$;
μ, dynamic viscosity;
v, kinematic viscosity $(= \mu/\rho)$;
ρ, density;
ξ, thickness ratio of transfer and velocity boundary layers $(= \Delta/\delta)$;
ϕ, angle from forward stagnation point.

† Atomic Energy Research Institute, Seoul, Korea.
‡ Department of Mechanical Engineering, University of Liverpool, England.

Subscripts

0,	value at stagnation point;
s,	value in stream outside the boundary layer;
w,	value at the surface;
∞,	free stream condition far removed from surface;
theo.,	theoretical;
f,	front half of sphere, $\phi = 0$–$90°$;
r,	rear half of sphere, $\phi = 90°$–$180°$;
wake,	wake of sphere;
l,	boundary-layer region;
t,	pertaining to total surface of sphere.

Barred quantities refer to average values.

1. INTRODUCTION

CONSIDERABLE attention has already been given to the experimental and theoretical determination of heat or mass transfer from bodies of spherical shape. Many practical engineering situations are readily called to mind. For example, heat transfer from the forward half of a sphere is of direct interest to the aerodynamicist [1], while a knowledge of the distribution of local transfer rates around a sphere is required in spherical fuel element applications in nuclear reactor engineering [2, 3, 4].

Many more examples are to be found particularly in the field of chemical engineering [5, 6].

The theoretical analysis of the transport processes from a sphere which is immersed in a fluid stream is based on the solution of the momentum, energy and mass conservation equations in axisymmetric flow. Frössling [7] made a theoretical study of the rotationally symmetrical laminar boundary-layer flow and obtained an exact solution. The local Nusselt number on the surface of a sphere was calculated by Merk [8] using the "wedge type flow" method, while Sibulkin [9] gave an exact treatment of heat transfer near the front stagnation point, the latter being a special case of the results by Frössling [7]. The von Kármán–Pohlhausen integral method for the solution of boundary-layer flows has been employed by Frössling [7] and Spalding [10] to calculate the Nusselt number. A similar method was adopted by Brown *et al.* [4] in their study of heat transfer from the front half of a sphere with constant heat flux, fourth and third order polynomials being employed for the velocity and temperature distributions respectively.

In the present investigation, integrated boundary-layer equations are solved using "quartics" for the velocity, temperature and concentration profiles from the forward stagnation up to the point of separation. In this way, the development of the diffusion (or thermal) boundary layer is calculated for an "isothermal" sphere for various values of the Schmidt (or Prandtl) number.

The experimental work is described in a later section. It suffices here to say that a method "dry-spraying" of napthalene was employed to measure directly the local mass-transfer rates around the sphere. This technique is used in studies in fluid mechanics to visualize boundary-layer transition.

2. BASIC EQUATIONS AND THEORETICAL CONSIDERATIONS

The appropriate integrated boundary-layer equations for axisymmetric flow (see e.g. [7] and [12]) may be expressed in dimensionless form as

$$\frac{1}{r}\frac{\mathrm{d}}{\mathrm{d}x}\left[r\int_0^{\Delta} u(1-\theta')\,\mathrm{d}y\right] = \alpha\left(\frac{\partial\theta'}{\partial y}\right)_w \qquad (1)$$

and

$$\frac{1}{r}\frac{\mathrm{d}}{\mathrm{d}x}\left[r\int_0^{\Delta} u(1-\beta)\,\mathrm{d}y\right] = D\left(\frac{\partial\beta}{\partial y}\right)_w. \qquad (2)$$

Because equations (1) and (2) are similar, a calculation need only be made for one or other of the potentials, and in this case, equation (2) which pertains to mass transfer has been chosen. In order to solve this equation, it is generally assumed that the potential profiles in laminar

flow are simple functions of wall distance [4, 7, 12, 13] and in the present work fourth order polynomials (following Tomotika [13]) have been selected for the velocity and concentration distributions. The procedure for the solution of the equation for the particular boundary conditions is familiar and only a brief outline is considered to be necessary here.

3. FORMATION OF EQUATIONS

(a) *Case* 1: *hydrodynamic boundary-layer thickness,* $\delta >$ *transfer boundary-layer thickness,* Δ

On introducing the appropriate expressions for the velocity u/U, and concentration, β, profiles and with $\delta > \Delta$, equation (2) may be written as

$$\frac{1}{r}\frac{\mathrm{d}}{\mathrm{d}x}[rU\delta f_1(\lambda, \xi)] = \frac{2D}{\delta\xi} \tag{3}$$

where

$$f_1(\lambda, \xi) = \left[\left(\frac{2}{15} + \frac{\lambda}{90}\right)\xi^2 - \left(\frac{\lambda}{84}\right)\xi^3 - \left(\frac{3}{140} - \frac{3\lambda}{560}\right)\xi^4 + \left(\frac{1}{180} - \frac{\lambda}{1080}\right)\xi^5\right].$$

Further manipulation of this equation results in

$$\frac{\mathrm{d}\xi}{\mathrm{d}\phi} = \frac{1}{\lambda f_2(\lambda, \xi)\, Sc}\cdot\frac{U'}{U} - \frac{U'}{2U}\frac{f_1(\lambda, \xi)}{f_2(\lambda, \xi)}\left(\frac{1}{r}\frac{\mathrm{d}r}{\mathrm{d}\phi}\cdot\frac{U}{U'}\right)\xi - \frac{f_1(\lambda, \xi)}{2f_2(\lambda, \xi)}\cdot\frac{U'}{U}\cdot\xi - \frac{f_1(\lambda, \xi)}{4f_2(\lambda, \xi)}\cdot\frac{\mathrm{d}Z}{\mathrm{d}\phi}\cdot\frac{\xi}{Z}$$
$$- \frac{f_3(\xi)}{f_2(\lambda, \xi)}\cdot\frac{U'}{U_\infty}\cdot\frac{\mathrm{d}Z}{\mathrm{d}\phi} - \frac{f_3(\xi)}{f_2(\lambda, \xi)}Z\cdot\frac{U''}{U_\infty} \tag{4}$$

where

$$f_2(\lambda, \xi) = \left(\frac{2}{15} + \frac{\lambda}{90}\right)\xi^2 - \frac{\lambda}{56}\xi^3 - \left(\frac{3}{70} - \frac{3\lambda}{280}\right)\xi^4 + \left(\frac{1}{72} - \frac{\lambda}{432}\right)\xi^5$$

$$f_3(\xi) = \frac{\xi^3}{180} - \frac{\xi^4}{168} + \frac{3\xi^5}{1120} - \frac{\xi^6}{2160}$$

and the parameter Z [13] is given by

$$Z = U_\infty\delta^2/Rv.$$

In his study of the laminar boundary layer on a sphere, Tomotika [13] used the momentum integral equation to calculate δ from the following differential equation

$$\frac{\mathrm{d}Z}{\mathrm{d}\phi} = \frac{U_\infty}{U}\cdot f(\lambda) - \frac{\cos\phi}{\sin\phi}\cdot\frac{U_\infty}{(\mathrm{d}U/\mathrm{d}\phi)}\cdot f^*(\lambda) + Z^2\cdot\frac{1}{U_\infty}\frac{\mathrm{d}^2U}{\mathrm{d}\phi^2}g^*(\lambda). \tag{5}$$

(For expressions for $f(\lambda)$, $f^*(\lambda)$, and $g^*(\lambda)$ see [13].) In the present study, equations (4) and (5) were solved simultaneously using the velocity distribution U/U_∞ [13] which was based on Fage's [14] experimental pressure distribution.

In the vicinity of the stagnation point, i.e. $\phi \to 0$ the following simplified equation is obtained

$$f_1(\lambda, \xi)\,\lambda\,.\,\xi = 1/Sc \tag{6}$$

which, with $\lambda = 4{\cdot}71601$ at $\phi = 0$, [13], may be solved by iteration.

(b) *Case* 2: *hydrodynamic boundary-layer thickness,* $\delta <$ *transfer boundary-layer thickness,* Δ

After similar steps are taken as outlined in case 1, the following result for ξ with $\delta < \Delta$ is obtained

$$\frac{d\xi}{d\phi} = \frac{1}{f_5(\lambda, \xi)}\left[\frac{1}{ZSc}\cdot\frac{U_\infty}{U} - \left(\frac{\cot\phi}{2} + \frac{U'}{2U} + \frac{1}{4Z}\cdot\frac{dZ}{d\phi}\right)\cdot f_4(\lambda, \xi)\,\xi - \left(\frac{U'}{U_\infty}\cdot\frac{dZ}{d\phi} + \frac{Z}{U_\infty}\frac{d^2U}{d\phi^2}\right) f_6(\xi)\right] \tag{7}$$

where

$$f_4(\lambda, \xi) = \frac{3\xi}{10} + \left(\frac{\lambda}{120} - \frac{3}{10}\right) - \frac{1}{\xi}\left(\frac{\lambda}{180} - \frac{2}{15}\right) + \frac{1}{\xi^3}\left(\frac{\lambda}{840} - \frac{3}{140}\right) - \frac{1}{\xi^4}\left(\frac{\lambda}{3024} - \frac{1}{180}\right)$$

$$f_5(\lambda, \xi) = \frac{3\xi}{20} + \frac{1}{\xi}\left(\frac{\lambda}{360} - \frac{1}{15}\right) - \frac{1}{\xi^3}\left(\frac{\lambda}{560} - \frac{9}{280}\right) + \frac{1}{\xi^4}\left(\frac{\lambda}{1512} - \frac{1}{90}\right)$$

$$f_6(\xi) = \frac{\xi}{240} - \frac{1}{360} + \frac{1}{1680\xi^2} - \frac{1}{6048\xi^3}.$$

Equation (7) was also solved with equation (5) by numerical methods to obtain the relative magnitudes of the boundary-layer thicknesses.

(c) *Case* 3: *hydrodynamic boundary-layer thickness,* $\delta \gg$ *transfer boundary-layer thickness,* Δ

For this condition, it is readily shown that

$$\frac{d(\xi^3)}{d\phi} = 3\left[\frac{1}{f_7(\lambda)\,.\,Sc\,.\,Z}\cdot\frac{U_\infty}{U} - \left(\frac{\cot\phi}{2} + \frac{U'}{2U} + \frac{1}{4Z}\,\frac{dZ}{d\phi} + \frac{1}{180 f_7(\lambda)}\cdot\frac{U'}{U_\infty}\cdot\frac{dZ}{d\phi} + \frac{Z}{180 f_7(\lambda)}\cdot\frac{U''}{U_\infty}\right)\xi^3\right] \tag{8}$$

where

$$f_7(\lambda) = \left(\frac{2}{15} + \frac{\lambda}{90}\right).$$

At $\phi = 0$ the following simplified expression results

$$\xi = \frac{1}{0{\cdot}9568\sqrt[3]{Sc}}. \tag{9}$$

Following the usual procedure, equation (8) was solved simultaneously with equation (5).

4. RESULTS OF THE NUMERICAL SOLUTION

The results of the calculation of the thickness ratio at the forward stagnation point for various values of the Schmidt (or Prandtl) number, are presented in Fig. 1. Values of ξ were determined from equations (4), (7) and (9) corresponding to the cases $\delta > \Delta$, $\delta < \Delta$ and $\delta \gg \Delta$ as $\phi \to 0$.

The Schmidt number for which ξ_0 becomes unity is calculated as 1·583 and it can be seen that the assumption that the thickness ratio is a function of $(Sc^{0.33})$ appears to be a fairly good approximation for values of $Sc > 10$.

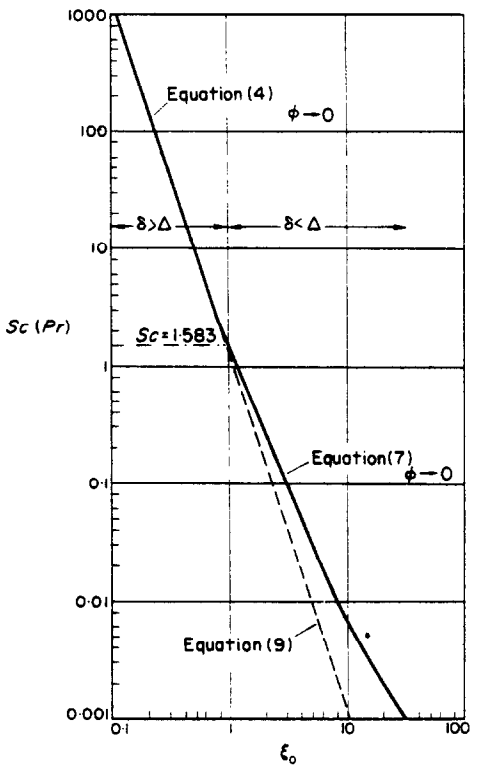

FIG. 1. Boundary-layer thickness ratio at the forward stagnation point.

The numerical values of ξ were normalized using the value at the forward stagnation point with the result shown in Fig. 2 where the ratio (ξ/ξ_0) is plotted versus the angular position for various values of Schmidt (or Prandtl) number. This plot suggests that the local transfer coefficient is a function of the Schmidt (or Prandtl) number in addition to the Reynolds number.

The local Sherwood number, Sh, may be defined as

$$Sh = \frac{h_D d}{D} = \left(\frac{\partial \beta}{\partial y'}\right)_w. \tag{10}$$

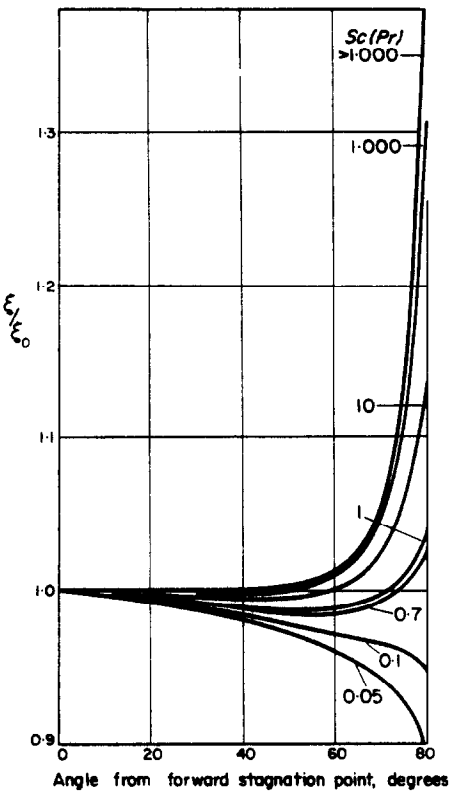

FIG. 2. Variation of boundary-layer thickness ratio with angular position.

Equation (10) can be developed further to obtain

$$Sh = \frac{2d}{\Delta} = \frac{2d}{\xi\delta}. \tag{11}$$

However, with the expression for Z equation (11) becomes

$$\frac{Sh}{Re^{0.5}} = \frac{2{\cdot}8284}{\xi Z^{0.5}}. \tag{12}$$

When $\delta \gg \Delta$ from equations (11) and (9) the Sherwood number becomes a function of $Sc^{0.33}$ as

$$\frac{Sh}{Re^{0.5}.Sc^{0.33}} = \frac{2{\cdot}7062}{Z^{0.5}}. \tag{13}$$

The local Sherwood number was calculated

from equation (12) and the results are given in Fig. 3 with the angle ϕ as a parameter. The local Nusselt number for a sphere was determined by Merk [8] using the wedge solution method and his results are compared with the present findings in Fig. 4. The agreement is remarkably good in the range $\phi = 0 \rightarrow$ about 70°.

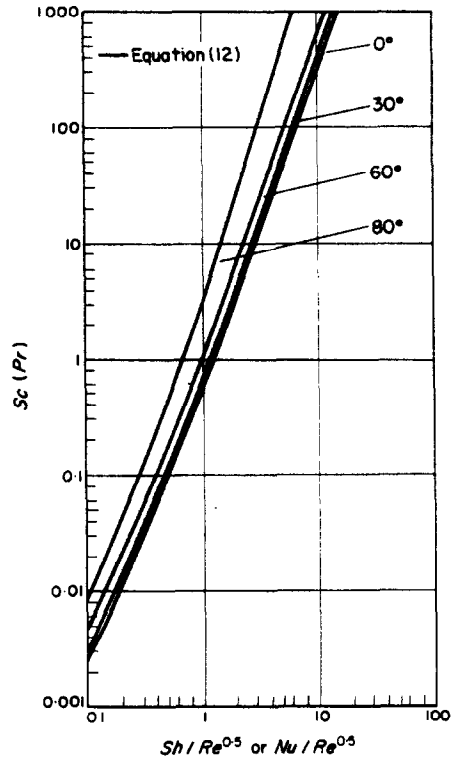

FIG. 3. Variation of local Sherwood (Nusselt) number against Schmidt (Prandtl) number.

The distribution of the local Sherwood number for the case $\delta \gg \Delta$, when equation (13) pertains, was compared with Merks [8] result as shown in Fig. 5. Again Merk's results follow closely the present prediction up to a value of ϕ equal to about 70°.

Finally, the normalized Sherwood numbers were plotted as indicated in Fig. 6. As mentioned earlier, the dependency of the local transfer coefficient on Schmidt (or Prandtl) number is readily apparent.

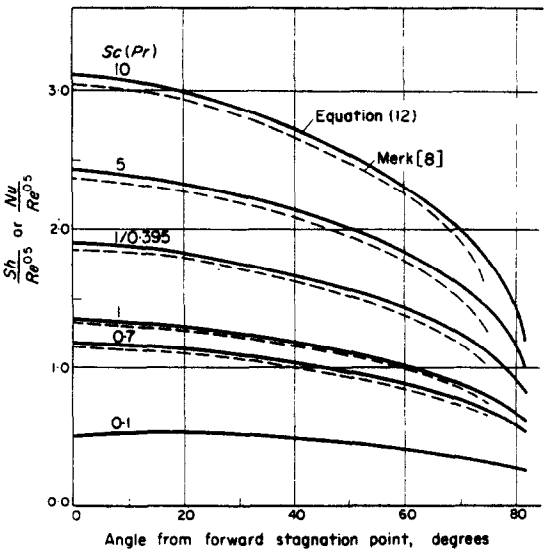

FIG. 4. The local Sherwood (or Nusselt) number for spheres

5. EXPERIMENTAL APPARATUS AND PROCEDURE

The experimental apparatus consisted of a napthalene coated sphere located in near uniform velocity air stream which was produced by flow near the inlet of a 5·6 in I.D. perspex tube. The effect of finite duct size on the local stream velocity was accounted for in the evaluation of

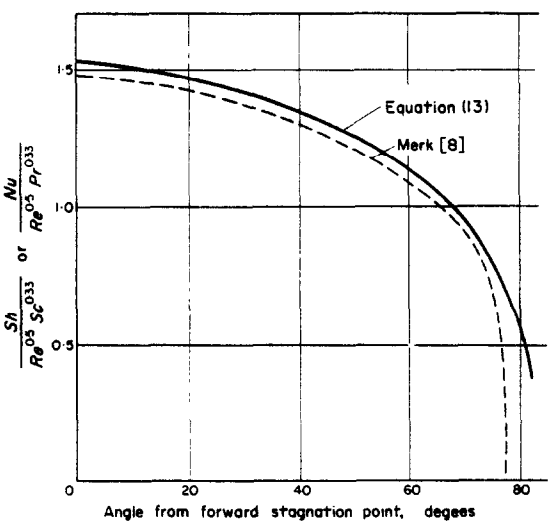

FIG. 5. The local Sherwood (or Nusselt) number for spheres when $\delta \gg \Delta$.

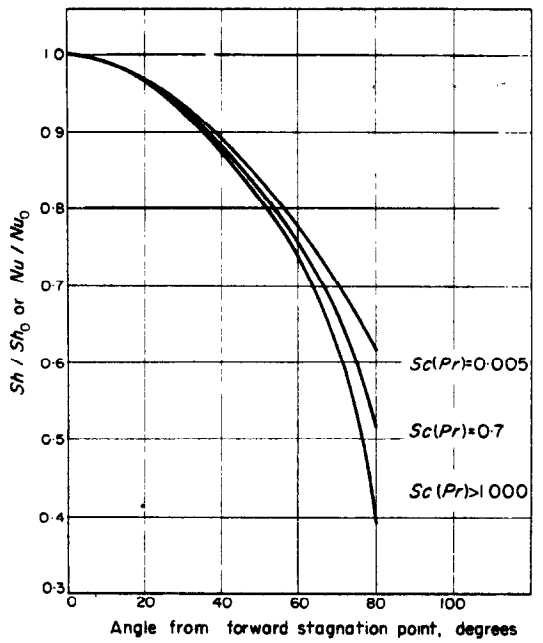

FIG. 6. Relative local Sherwood (or Nusselt) number.

the results. The test spheres, which were made from $1\frac{1}{4}$-in dia. and $\frac{7}{8}$-in dia. ball bearings mounted on small diameter spindles, were located 14 in from the bell mouth entry to the tube. The spindle supporting the test sphere was perpendicular to the air flow in all tests.

The napthalene coating was produced by a "dry-spraying" technique. With the correct solution and spraying distance, napthalene can be deposited uniformly on the surface of the sphere in a dry state. The spraying solution in the present experimental work was produced by dissolving 2 g of "organic analytical standard" napthalene in 100 ml acetone. With suitable spraying conditions, the deposited napthalene had a density of approximately one half that of solid napthalene.

After spraying, the diameter of the equator of the sphere in the plane perpendicular to the spindle was measured in a "matrix floating carriage diameter measuring machine". The sphere was then located in the duct so that the point where the change in thickness of the coating was to be measured was at the required angular position relative to the flow direction. Exposure times to air flow varied from 20 to 40 min for each measurement. After exposure, the diameter was measured again to determine the change in thickness of the napthalene deposit. The surface of the sphere at a point diametrically opposite to that being studied was cleaned to facilitate the thickness measurements. The range of Reynolds number studied was 3199–25350, five to twenty-six mass-transfer measurements being correlated to represent an experimental Sherwood number for each angular position.

6. EXPERIMENTAL RESULTS

The experimental values of the local Sherwood number have been plotted vs. the angle from the forward stagnation point in Fig. 7. The distribution of mass-transfer rate is similar to that which has been observed by the present authors [15] in some earlier experiments using chemical methods to visualize the phenomenon.

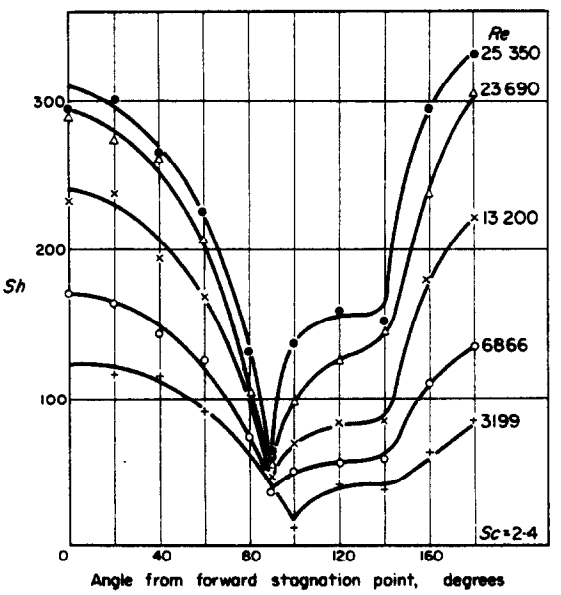

FIG. 7. Experimental local Sherwood number around a sphere.

The significant reduction in mass-transfer rate in the region $\phi = 70 \rightarrow 140°$ is clearly seen in Fig. 7.

The experimental results for the front half of the sphere are compared with the prediction of the laminar boundary-layer analysis in Fig. 8. Although the scatter of the data is noticeable, the agreement between theory and experiment is fairly good. The theoretical local Nusselt number for $Pr = 0{\cdot}7$ is compared with the experimental data of Short *et al.* [16], Hsu *et al.* [17] and Xenakis *et al.* [18] with the result shown in Fig. 9. The measurements made by Xenakis *et al.* [18] are in good agreement with the theoretical prediction for the case of very large Prandtl (or Schmidt) number.

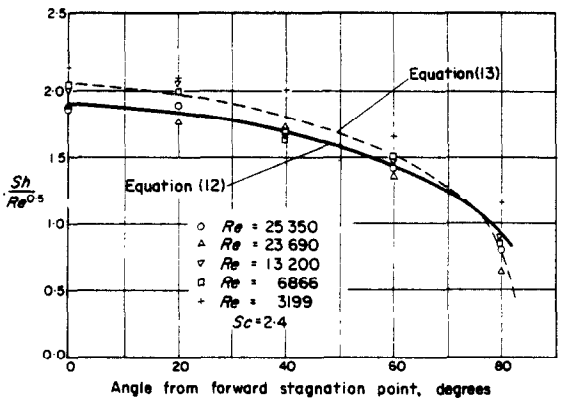

FIG. 8. Comparison of theoretical and experimental local Sherwood number in boundary-layer flow.

The comparison made in Fig. 9, however, pertains to gas flows, so that the theoretical result for the case of Pr very large is not relevant.

The results of the present experimental study show a point of separation at or around 90° whereas the point of separation according to the theory using the velocity equation obtained by Tomotika [13] is at about 82°. It might be that the semi-theoretical equation for the velocity distribution does not describe exactly the velocity distribution in the present tests.

7. AVERAGE SHERWOOD NUMBER OVER THE FRONT HALF OF THE SPHERE

The experimental local Sherwood number was integrated graphically over the front half of the sphere to obtain an average Sherwood number weighted for area. The experimental values which were obtained by Frössling [19] from experiments with napthalene balls for $Re = 136$–1060 were also averaged by graphical methods. The two sets of results are shown in Fig. 10. The average Sherwood number was then correlated by the equation

$$\overline{Sh}_f = 1{\cdot}02\, Re^{0{\cdot}5}\, Sc^{0{\cdot}33} \qquad (14)$$

over the range of $Re = 136$–25350.

The theoretical local Sherwood number for napthalene, which was originally calculated up to $\phi = 82°$, was extrapolated to encompass the

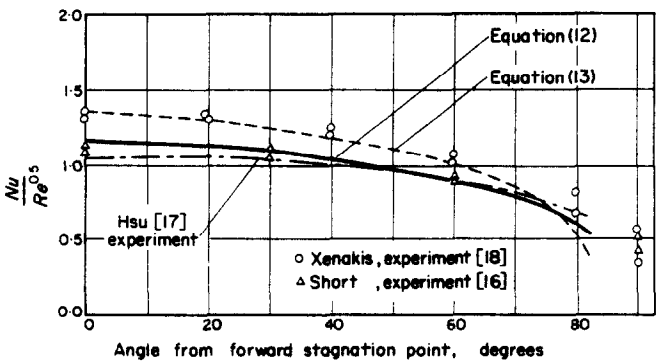

FIG. 9. Local heat-transfer coefficient in laminar flow ($Pr = 0{\cdot}7$).

whole of the front half of the sphere and graphical integration resulted in

$$\overline{Sh}_{f,\text{theo}} = 0{\cdot}976\, Re^{0{\cdot}5}\, Sc^{0{\cdot}33}. \qquad (15)$$

Clearly there is excellent agreement between theory and experiment. Further evidence of the accuracy of the experimental correlation, equation (14), and its supporting theoretical prediction, equation (15), is the good agreement of Xenakis's [18] heat-transfer results at the upper end of the Reynolds number range.

by

$$\overline{Sh}_r = 0{\cdot}0447\, Re^{0{\cdot}78}\, Sc^{0{\cdot}33}. \qquad (16)$$

A further comparison is made in Fig. 11 where the ratio $\overline{Sh}_f/\overline{Sh}_r$ has been plotted versus the Reynolds number. The correlation

$$\overline{Sh}_f/\overline{Sh}_r = 22{\cdot}8\, Re^{-0{\cdot}28} \qquad (17)$$

is good and can be seen to fit the present data, that of Frössling [19] and the heat-transfer results of Xenakis *et al.* [18] satisfactorily. It is

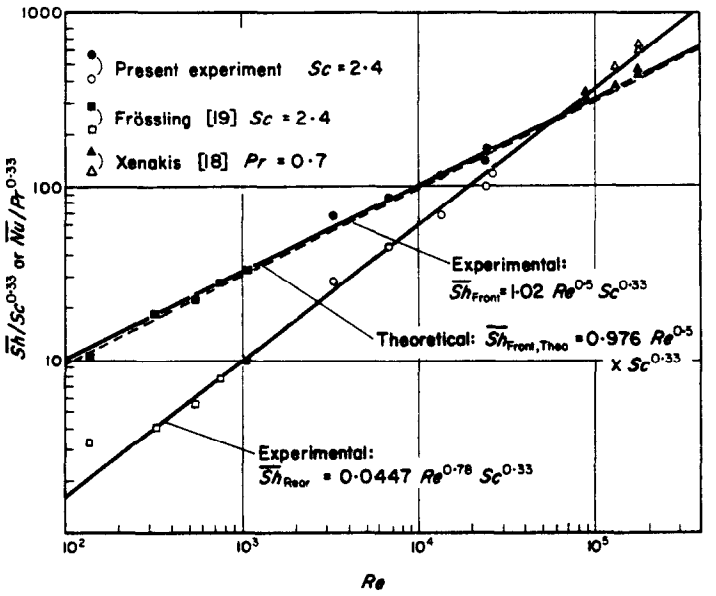

FIG. 10. Average Sherwood (Nusselt) number for the front (0–90°) and the rear (90–180°) of a sphere.

8. SEPARATED FLOW REGION

(a) *Average transfer rates over the rear half of the sphere*

The average experimental mass-transfer rates over the rear half of the sphere (ϕ = 90–180°) were obtained by graphical integration. These have been plotted, along with the corresponding results of Frössling [19], in Fig. 10 for comparison with the data for the front half of the sphere. The whole of the data are well correlated surprising that a single correlation for the transfer rate over the rear half of the sphere is possible over the Reynolds number range $2 \times 10^2 \rightarrow 2 \times 10^5$. However, the results presented in both Figs. 10 and 11 have to be considered in two separate parts according to the value of the Reynolds number. For $Re >$ 2000, the experimental results of this study indicate boundary-layer separation at about 90° from the forward stagnation point, so that

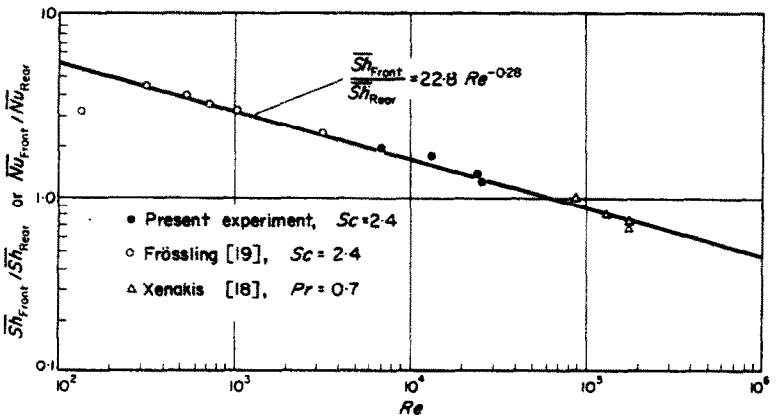

FIG. 11. Sherwood (or Nusselt) number ratio for front (0–90°) and rear (90–180°) of a sphere.

$\overline{Sh}_r = \overline{Sh}_{wake}$ and equation (16) may be written as

$$\overline{Sh}_{wake} = 0{\cdot}0447\ Re^{0{\cdot}78}\ Sc^{0{\cdot}33} \qquad (18)$$

$$\text{for} \quad 2000 < Re < 20000.$$

For lower Reynolds numbers, the point of separation depends on the Reynolds number as shown in Fig. 12. Therefore, the average Sherwood numbers for the rear half (i.e. $\phi = 90$–$180°$) given by equation (16) includes both the contributions of the wake and the boundary-layer flow between 90° and the point of separation. Because of the change of the wake area, it is difficult to estimate the separation effect of the wake directly from equation (16).

(b) *Transfer processes in the wake region*

The position of boundary-layer separation moves upstream with increase in Reynolds number in the lower Reynolds number range. From the present experiments with the mass transfer of napthalene and with the data of Frössling [19], the angular position of the point of separation is approximately a function of $(Re^{-0{\cdot}1})$ according to Fig. 12. In Fig. 13 the average Sherwood numbers which have been obtained in the present investigation for the boundary-layer and wake regions are presented along with the results of Frössling [19] and Xenakis *et al.* [18]. This plot is not to be confused with that of Fig. 10 where the average Sherwood numbers were considered for the front and rear halves of the sphere separately. In Fig. 13 the average Sherwood numbers for the boundary-layer region (variable area) and the wake region (variable area) are given. It is to be noted at this point that when $Re >$ about 2000, Figs. 10 and 13 become identical because the wake area is essentially constant. Several

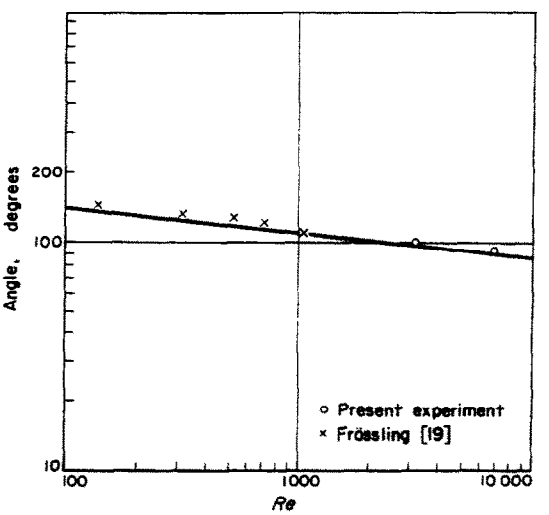

FIG. 12. Position of separation with naphthalene experiments.

interesting features are to be observed from Fig. 13.

Firstly, it was shown in [20] that the assumption of a "wake boundary layer" for very small Reynolds numbers is justified in the immediate neighbourhood of the rear stagnation point. In other words, for small values of Re, the transfer coefficient may be expressed as a function of $Re^{0.5}$. Returning to our considerations of Fig. 13 it is to be observed that when $Re < 500$ the average Sherwood number for the wake is well represented as a function of $Re^{0.5}$ as

$$\overline{Sh}_{\text{wake}} = 0.175\, Re^{0.5}\, Sc^{0.33} \qquad (19)$$

$$\text{for} \quad 100 < Re < 500.$$

Secondly, as earlier observations [20] indicate, the decrease in the stability of the "wake boundary layer" with increase in Reynolds number promotes the transfer rate in the wake. Figure 13 is in accordance with this idea in that the average Sherwood number is a function of $Re^{0.78}$ when Re exceeds about 2000.

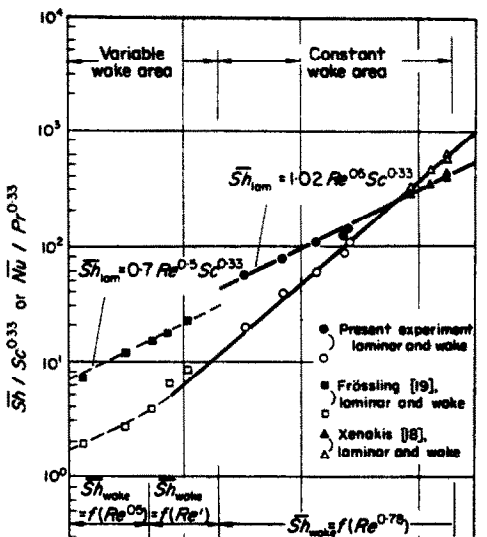

FIG. 13. Average Sherwood (Nusselt) number for laminar and wake regions of a sphere.

Finally, for $Re < 2000$, the area encompassing the boundary layer increases with decrease in Re, and yet the average value of Sh remains a function of $Re^{0.5}$ as shown in Fig. 13. However, because of the increase of the surface area in the vicinity of smaller local Sherwood number, the average value is reduced below that given in Fig. 10 for constant wake area and the following equation represents $\overline{Sh}$ for the laminar region over the range $100 < Re < 2000$.

$$\overline{Sh}_l = 0.7\, Re^{0.5}\, Sc^{0.33}. \qquad (20)$$

(c) *The nature of the wake*

The nature of the wake in regard to transfer processes may best be represented by three distinct regimes according to the hydrodynamic conditions near the surface in the wake. This conclusion has been reached as a result of the earlier observations of the present writers [20] and the present napthalene experiments. The three regimes are described as follows:

(i) The "wake boundary layer" flow regime

$$\overline{Sh}_{\text{wake}} = f(Re^{0.5}), \qquad 100 < Re < 500.$$

(ii) The "intermediate" flow regime

$$\overline{Sh}_{\text{wake}} = f(Re^{i}), \qquad 500 < Re < 2000$$

where i increases with increase in Re ($0.5 \leqslant i \leqslant 0.78$).

(iii) The "final" flow regime

$$\overline{Sh}_{\text{wake}} = f(Re^{0.78}), \qquad 2000 < Re < 200000.$$

The above classification gives a clearer picture of the contribution of the wake flow to the overall transfer rate. In a review of heat-transfer results in separated flows by Hanson and Richardson [21], reference was made to an earlier conclusion made by the second author. He concluded that heat and mass transfer in a separated flow was proportional to the Reynolds number to the two-thirds power, which is about the average of the range of the exponent of Re given in (i), (ii) and (iii) previously. Any difference

between the exponent of the Reynolds number given here and those of other studies at a particular value of Re is possibly due to the intensity of turbulence in the free stream in the experimental work.

In the past, there have been considerable differences of opinion concerning the exponents of the Reynolds numbers in overall heat- and mass-transfer correlations. For example, Yuge [22] gave 0·5 for the exponent for $10 < Re < 1{\cdot}8 \times 10^3$ and 0·5664 for $1{\cdot}8 \times 10^3 < Re < 1{\cdot}5 \times 10^5$ in his equations for the Nusselt number. Brown *et al.* (4) recommended 0·6 for $5000 < Re < 480000$ while Frössling [19] and Ranz and Marshall [23] proposed an exponent of 0·5 for small Reynolds numbers. At lower Reynolds numbers, the contributions of the wake is small and most of the transfer occurs in the boundary-layer flow, when the overall Sherwood number may well be expressed as a function of $Re^{0.5}$. This is true for most of the overall heat- and mass-transfer correlations at small Reynolds numbers. With increasing values of Re, however, the transfer rate in the wake becomes more significant and this is reflected in an increase in the exponent of Re as indicated under (i–iii) above. The general trend of the suggested correlations for the wake region are therefore compatible with the observations on overall transfer coefficients.

9. THE OVERALL TRANSFER COEFFICIENT

The average Sherwood numbers for the boundary layer and wake regions may be combined to obtain an overall mass-transfer coefficient for the sphere. The average Sherwood number for the front according to equation (14) was combined with that for the rear according to equation (16) to give the following empirical relation over the Reynolds number range $200 \rightarrow 200000$

$$\overline{Sh}_t \,.\, Sc^{-0.33} = 0{\cdot}51\, Re^{0.5} + 0{\cdot}02235\, Re^{0.78}. \tag{21}$$

Equation (21) is shown in Fig. 14 together with various other recommended correlations and experimental data. It is seen that the experimental data of Xenakis *et al.* [18] is in excellent agreement as mentioned earlier. The equation for heat transfer to water from an isothermal sphere due to Vliet and Leppert [3] agrees very well with the present equation for Re between 1000 and 20000. The correlation proposed by

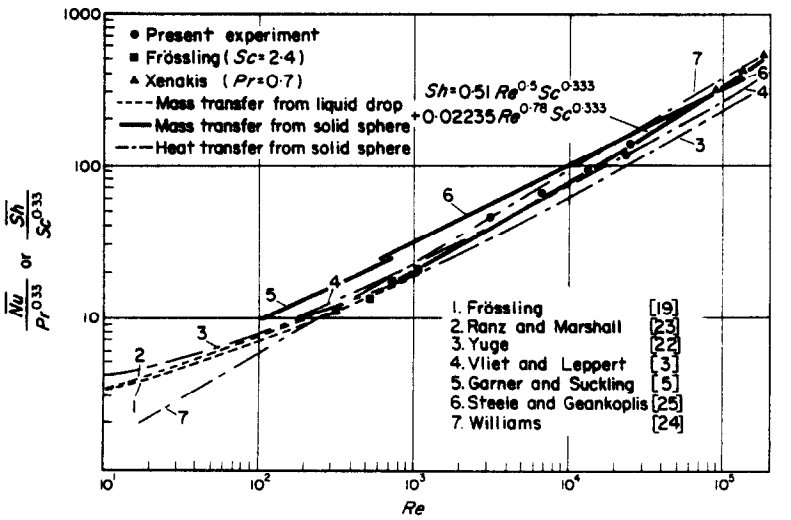

FIG. 14. Overall heat- and mass-transfer coefficient from a sphere.

Williams [24] for heat transfer to air lies above equation (21) with a larger slope, and that of Yuge [22] lies below with a smaller slope. In either case, the agreement with the present correlation is good at small Reynolds numbers. Several other heat-transfer results fall, in general, between the recommendations of [22] and [24]. The experiments of Garner and Suckling [5], and Steele and Geankoplis [25] were conducted using values of Sc equal to 1000 and above; it is interesting to note that their recommendations are noticeably in excess of those of the other investigators and the result given here. It might be that the present result is least accurate at very large values of the Schmidt number and some correction needs to be made to equation (21) to meet this case.

10. CONCLUSION

An investigation of local and average transfer rates from the surface of a sphere has been made. New experimental data on local mass transfer for Reynolds numbers varying from 3199 to 25350 have been obtained from experiments with the sublimation of napthalene from the surface.

The experimental data for the laminar boundary-layer region have been compared with the results of a theoretical analysis which uses the integral method. Both local and averaged mass-transfer coefficients are predicted well by the theory; the average mass-transfer coefficient, which is weighted for area, is within $4\frac{1}{2}$ per cent of the corresponding experimental value.

In the separated flow region, the exponent of the Reynolds number in the Sherwood number, Schmidt number–Reynolds number relationship for the average mass-transfer coefficient is found to be dependent on the Reynolds number. The wake region study is therefore considered in three parts according to Reynolds number ranges which are identified with particular regimes of flow. The increase in the contribution of the wake to transfer with increasing Reynolds number is made manifest by an increase in the power of the Reynolds number; this is compatible with the increasing exponent of the Reynolds number in the correlations of other experimenters for overall transfer.

The experimental boundary layer and wake region mass-transfer coefficients when combined yield a correlation for the overall average Sherwood number which is in good agreement with other recommendations with the exception of some which pertain to very large values of the Schmidt number. The final correlation is applicable over the range of Reynolds number, $2 \times 10^2 \rightarrow 2 \times 10^5$.

REFERENCES

1. J. R. CARY, The determination of local forced convection coefficients for spheres, *Trans. Am. Soc. Mech. Engrs* **75**, 483–487 (1953).
2. J. WADSWORTH, The experimental examination of the local heat transfer on the surface of a sphere when subjected to forced convection cooling, Canadian National Research Council Report MT-39 (1958).
3. G. C. VLIET and G. LEPPERT, Forced convection heat transfer from an isothermal sphere to water, *J. Heat Transfer* **83**, 163–175 (1961).
4. W. S. BROWN, C. C. PITTS and G. LEPPERT, Forced convection heat transfer from a uniformly heated sphere, *J. Heat Transfer* **84**, 133–140 (1962).
5. F. H. GARNER and R. D. SUCKLING, Mass transfer from a soluble solid sphere, *A.I.Ch.E. Jl* **4**, 114–124 (1958).
6. R. L. STEINBERGER and R. È. TREYBAL, Mass transfer from a solid soluble sphere to a flowing liquid stream, *A.I.Ch.E. Jl* **6**, 227–232 (1960).
7. N. FRÖSSLING, Evaporation, heat transfer and velocity distribution in two-dimensional and rotationally symmetrical laminar boundary layer flow, Lunds Universitets Årsskrift N.F. avd. 2, 36, No. 4 (1940). English translation in NACA TM 1432 (1958).
8. H. J. MERK, Rapid calculations for boundary layer transfer using wedge solution and asymptotic expansions, *J. Fluid Mech.* **5**, 460–480 (1959).
9. M. SIBULKIN, Heat transfer near the forward stagnation point of a body of revolution, *J. Aeronaut. Sci.* **19**, 570–571 (1952).
10. D. B. SPALDING, Mass transfer in laminar flow. *Proc. R. Soc.* **A221**, 78–99 (1954).
11. J. D. MAIN SMITH, Chemical solids as diffusible coating film for visual indications of boundary layer transition in air and water, Brit. Aero. Res. Coun., R.M. No. 2755 (1950).
12. E. R. G. ECKERT and R. M. DRAKE, *Heat and Mass Transfer*. McGraw-Hill, New York (1959).
13. S. TOMOTIKA, Laminar boundary layer on the surface of a sphere in a uniform stream, Brit. Aero. Res. Com. R.M. No. 1678 (1935).

14. A. FAGE, Experiments on a sphere at critical Reynolds numbers, Brit. Aero. Res. Com. R.M. No. 1766 (1936).
15. K. LEE, H. BARROW and D. J. RYLEY, The visualisation of mass transfer rate around a sphere, *Jl R. Aeronaut. Soc.* **68**, 137–139 (1964).
16. W. W. SHORT, R. A. S. BROWN and B. H. SAGE, Thermal transfer in turbulent gas stream, effect of turbulence on local transport from spheres, *J. Appl. Mech.* **27**, 393–402 (1960).
17. N. T. HSU and B. H. SAGE, Thermal and material transfer in turbulent gas stream local transport from spheres, *A.I.Ch.E. Jl* **3**, 405–410 (1957).
18. G. XENAKIS, A. E. AMERMAN and R. W. MICHELSON, An investigation of the heat transfer characteristics of spheres in forced convection, Wright Air Development Center, Ohio, TR52-117 (April 1955).
19. N. FRÖSSLING, Über die Verdunstung Fallenden Tropfen, *Beitr. Geophys.* **52**, 170–216 (1938).
20. K. LEE and H. BARROW, Some observations on transport processes in the wake of a sphere in low speed flow, *Int. J. Heat Mass Transfer* **8**, 403–409 (1965).
21. F. B. HANSON and P. D. RICHARDSON, Mechanics of turbulent separated flows as indicated by heat transfer: a review, in *Symposium in Fully Separated Flows*, pp. 27–32. Am. Soc. Mech. Engrs, New York (1964).
22. Y. YUGE, Experiments on heat transfer from spheres including combined natural and forced convection, *J. Heat Transfer* **82**, 214–220 (1960).
23. W. E. RANZ and W. R. MARSHALL, JR., Evaporation from drops, *Chem. Engng Prog.* **48**, 141–146, 173–180 (1952).
24. H. I. WILLIAMS, *Heat Transmission*, edited by W. H. MCADAMS, 3rd edn., p. 237. McGraw-Hill, New York (1954).
25. L. R. STEELE and C. J. GEANKOPLIS, Mass transfer from a solid sphere to water in highly turbulent flow, *A.I.Ch.E. Jl* **5**, 178–181 (1959).

Résumé— Dans l'étude actuelle, les équations intégrales de la couche limite sont résolues pour calculer le développement de la couche limite de diffusion (ou thermique) à partir du point d'arrêt amont d'une sphère jusqu'au point de décollement, pour différents nombres de Schmidt (ou de Prandtl). Les profils polynomiaux de Pohlhausen sont employés pour décrire les formes des couches de transport dans la région laminaire.

Une méthode de "vaporisation à sec" de naphtalène a été employée pour déterminer expérimentalement le nombre local de Sherwood pour des nombres de Reynolds entre 3199 et 23350.

Les résultats expérimentaux pour la région laminaire sont comparés avec ceux en accord avec la théorie. Pour le sillage, une étude des données expérimentales montre qu'il est possible de remarquer trois régimes distincts correspondant à différentes gammes de nombres de Reynolds.

Les résultats actuels sont combinés avec ceux d'autres expérimentateurs pour le transport de chaleur et de masse afin d'obtenir un coefficient de transport global à partir d'une sphère pour une gamme de nombres de Reynolds de 2000 à 200000.

Zusammenfassung—In der vorliegenden Arbeit werden die integrierten Grnezschichtgleichungen gelöst, um die Entwicklung der Diffusions- (oder thermischen) Grenzschicht zu berechen vom vorderen Staupunkt einer Kugel bis zum Ablösungspunkt, bei verschiedenen Werten der Schmidt- (oder Prandtl) Zahl. Zur Beschreibung der Formen der Übergangsschichten im Laminarbereich wurden Pohlhausen-Polynomprofile verwendet.

Eine "Trockensprühmethode für Naphtalin diente zur experimentellen Bestimmung der örtlichen Sherwood-Zahl für Reynolds-Zahlen von 3199 bis 25350. Die Ergebnisse der Versuche für den Laminarbereich werden mit jenen der Theorie verglichen. Eine Betrachtung der Versuchswerte zeigt, dass im Nachlauf, entsprechend den unterschiedlichen Reynolds-Zahlen, drei getrennte Regime unterschieden werden können.

Die hier erhaltenen Ergebnisse sind mit Ergebnissen anderer Experimentatoren kombiniert um einen Gesamtübergangskoeffizient von einer Kugel im Bereich von Reynolds-Zahlen von 200 bis 200000 zu erhalten.

Аннотация—В данной статье решаются интегральные уравнения пограничного слоя для расчета формирования диффузионного (или теплового) пограничного слоя от передней критической точки шара до точки отрыва при различных значениях числа Шмидта (или Прандтля). Профили даются в виде полинома Польгаузена для изучения переноса в ламинарной области.

Для экспериментального определения локального числа Щервуда в диапазоне изменения чисел Рейнольдса от 3199 до 25350. Применялся метод «сухого распыления» нафталина.

Экспериментальные результаты по ламинарному режиму сравнивались с теоретическими. Эксперимент показал, что три области отрыва соответствуют различным диапазонам изменения чисел Рейнольдса.

Полученные данные сравниваются с другими исследованиями по тепло-и массообмену с целью получения среднего коэффициента теплообмена от шара в диапазоне изменения чисел *Re* от 200 до 200000.